ELSEVIER

Optics and Lasers in Engineering 37 (2002) 51–62

OPTICS and LASERS in ENGINEERING

Fringe skeletonizing using an improved derivative sign binary method

Dongsheng Zhang[a,*,1], Min Ma[a], Dwayne D. Arola[b]

[a] *Department of Astronautical Technology, National University of Defense Technology, Changsha, People's Republic of China, 410073*

[b] *Department of Mechanical Engineering, University of Maryland Baltimore County, 1000 Hilltop Circle, Baltimore, MD 21250, USA*

Received 1 December 2000; received in revised form 1 May 2001; accepted 1 August 2001

Abstract

A modified derivative sign binary method is proposed to extract fringe skeletons from interferometric fringe patterns. A fringe direction map ranging from 0° to 360° is obtained with an unambiguous relationship between the grayscale and fringe tangent direction. Using this approach, the derivative sign binary map is detected without a fringe direction jump. The dark (light) fringe intensity minimum (maximum) can be extracted automatically to define fringe skeletons. In addition, two different anisotropic one-dimensional filters are described that can be used for further improving the fringe quality. Examples are provided for a holographic interferogram and a Moiré fringe pattern to illustrate applications and benefits of the approach.

Keywords: Filter; Fringe patterns; Skeleton

1. Introduction

Although phase shifting and Fourier transforms are regularly enrolled for fringe pattern analysis, fringe skeletonizing is still one of the most important methods for processing interferograms. Fringe skeletonizing can be achieved using either the fringe tracking method (FTM) [1,2], the fringe binary method (FBM) [3–7], or the fringe orientation based method [7–12]. Although fringe skeletonization techniques

*Corresponding author.

E-mail address: donzhang@engr.umbc.edu (D. Zhang).

[1] Present address: Department of Mechanical Engineering, University of Maryland Baltimore County, 1000 Hilltop Circle, Baltimore, MD 21250, USA. Tel.: +1-410-455-3395; fax: +1-410-455-1052.

0143-8166/02/$ - see front matter
PII: S0143-8166(01)00148-8

are fairly well developed, a complete review of the literature in this area is beyond the scope of the present study. The FTM tracks the fringe patterns individually according to the minimum grayscale level existing at the dark fringe center. This process can be cumbersome for whole-field skeleton extraction. The FBM segments the dark fringe area according to a given threshold and a thinning algorithm is then implemented to obtain its geometric center. The geometric center is regarded as the dark fringe center but this assumption can give rise to errors if the fringe intensity is unsymmetric and the fringe intensity grayscale gradient is low. The optimum threshold can be hard to estimate when using the FBM due to non-uniform background intensity or in situations where fringe contrast is low. The fringe orientation method (FOM) is based on the construction of a fringe orientation map. With knowledge of fringe orientation, background noise can be reduced efficiently and a derivative sign binary map, with boundary between black and white representing the dark (light) fringe intensity minimum (maximum), can be deduced precisely. However, since the fringe orientation ranges from 0° to 180°, binary fringe jumps are caused by jumps in the fringe direction definitions. Although there are methods available to erase direction jump lines after skeleton extraction, fringe skeleton discontinuity often remains [10]. Therefore, an approach for obtaining the fringe orientation map is needed which is able to extend the range to 360° and omit the fringe skeleton discontinuity.

In this paper, an approach for constructing the fringe direction map is introduced with the range from 0° to 360°. The processing steps necessary for extracting the continuous fringe skeleton are described and an anisotropic filtering process used to improve the overall fringe quality is also presented.

2. Background

Prior to extracting skeletons, it is first necessary to determine and assign orientation to the fringes. The orientation (α) of a fringe pattern is perpendicular to the fringe grayscale gradient β, which can be defined by

$$\beta = \arctan \frac{g_y(r)}{g_x(r)}, \tag{1}$$

where $g_x(r)$ and $g_y(r)$ represent the gradient components at point r along the x and y axes, respectively. For ideal fringe patterns, these quantities are obtained from grayscale information according to

$$g_x(x, y) = \tfrac{1}{2}(\text{Grayscale}_{x+1,y} - \text{Grayscale}_{x-1,y}), \tag{2a}$$

$$g_y(x, y) = \tfrac{1}{2}(\text{Grayscale}_{x,y+1} - \text{Grayscale}_{x,y-1}). \tag{2b}$$

In practice, fringe patterns that result from the application of general optical methods (e.g. Moiré and holography) are treated using Eq. (2) after the noise suppression techniques have been applied. The fringe orientation (α) can be obtained

using Eq. (1) by adding or subtracting 90° from the known β. However, according to Eq. (1), and the definitions for $g_x(r)$ and $g_y(r)$ in Eq. (2), α is limited to the range $0^\circ \leqslant \alpha \leqslant 180^\circ$ and results in two fringe directions (α and $\alpha + 180^\circ$) for each grayscale. The actual range in α should be $0^\circ \leqslant \alpha \leqslant 360^\circ$, which supports a unique (or singular) relationship between the grayscale and fringe direction; an unambiguous relationship between these two quantities is required for efficient and accurate fringe post-processing.

Here, a quadratic energy function $U(p)$ called the Gauss–Markov measure field method (GMMFM) is adopted to extend the range of α to $0^\circ \leqslant \alpha \leqslant 360^\circ$. The GMMFM has been designed by the Bayesian estimation and the Markov Random-field theory and is described in detail in Ref. [13]. The energy function is given by

$$U(p) = \sum_S [(1 + C_{rs})(p_r - p_s)^2 + (1 - C_{rs})(p_r + p_s - 1)^2 + u(p_{r_0} - 1)^2] \tag{3}$$

and is defined over the whole image S. Note that s is the neighboring spatial location of point r, and p_r and p_s represent the probability of whether the fringe directions (γ_r and γ_s) are equal to $\alpha + 180^\circ$ at point r and s, respectively. Also, u is a large positive number, and $C_{rs} = \cos(\alpha_r - \alpha_s)$. According to statistical theory, the quadratic energy function ($U(p)$) has to be minimized. A set of linear equations can be obtained by setting $\partial U/\partial p_r = 0$ at all points in the image. For example, at any point r the partial derivative of Eq. (3) is defined at each adjacent point over the neighborhood (N) of 8 points (s) as

$$2\sum_{s \in N} [(1 + C_{rs})(p_r - p_s) + (1 - C_{rs})(p_r + p_s - 1)] + \delta_{r_0}\mu(p_{r_0} - 1)^2 = 0, \tag{4}$$

where

$$\delta_{r_0} = \begin{cases} 1 & \text{if } r = r_0, \\ 0 & \text{otherwise.} \end{cases}$$

Note that at each point (r), p_r is defined according to Eq. (4) in terms of the probability defined at each of the 8 neighboring pixels (s). By solving the series of equations defined for the whole image simultaneously, the probability (p_r) at every point in the image is calculated. The fringe direction (γ_r), which has unique relationship between grayscale and direction, can then be obtained from the probability p_r according to

$$\gamma_r = \begin{cases} \alpha_r, & p_r < 0.5, \\ \alpha_r + 180, & p_r \geqslant 0.5. \end{cases} \tag{5}$$

a direction should be chosen at an initial starting point r_0 to begin the algorithm.

An example of this process can be illustrated through application to an actual holographic fringe pattern image as shown in Fig. 1. It is important to reduce noise and increase the signal to noise ratio prior to implementing Eq. (1). Since the fringe orientation is not sensitive to edge blurring caused by filtering, a general average or median filter is applied first. The grayscale distribution along the radial direction of the interferogram in Fig. 1 is shown before and after filtering in Fig. 2(a) and (b),

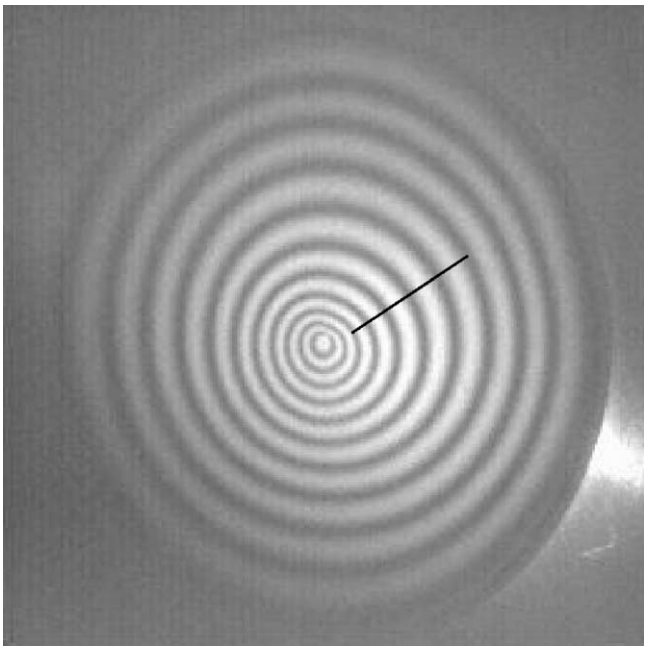

Fig. 1. A holographic fringe pattern. The grayscale distribution of the interferogram along the radial line highlight is shown in Fig. 2.

respectively, and the corresponding fringe orientation saw-tooth map is shown in Fig. 3. Note that each grayscale not only represents its specified direction but also represents the direction with 180° phase angle difference. For example, grayscale level 0 represents the positive and negative x-axes, when in fact this grayscale level should represent only one of these two directions according to its assignment.

The fringe orientation (from $0^\circ \leqslant \alpha \leqslant 180^\circ$) of the holographic interferogram is extended to the fringe direction ($0^\circ \leqslant \gamma_r \leqslant 360^\circ$) through further processing using Eq. (4). The initial starting point (r_0) for processing was chosen arbitrarily. The authors chose point (100,100) in which the fringe direction for this point and points in the surrounding neighborhood are in, and remain in, the range $0^\circ \leqslant \alpha \leqslant 180^\circ$. A complete fringe direction map for the interferogram in Fig. 1 is shown in Fig. 4. Each grayscale level represents a unique orientation defined clockwise from the x-axis. As the image dimension is 512×512 pixels, a series of 262,144 linear equations were solved to establish the fringe directions and required approximately 10 min of computation on a 800 MHz Pentium III desktop computer.

3. Anisotropic median and average filters

Although general median and average filters are used to remove noise, they can also cause blurring of the fringe pattern [14]. To avoid this problem the

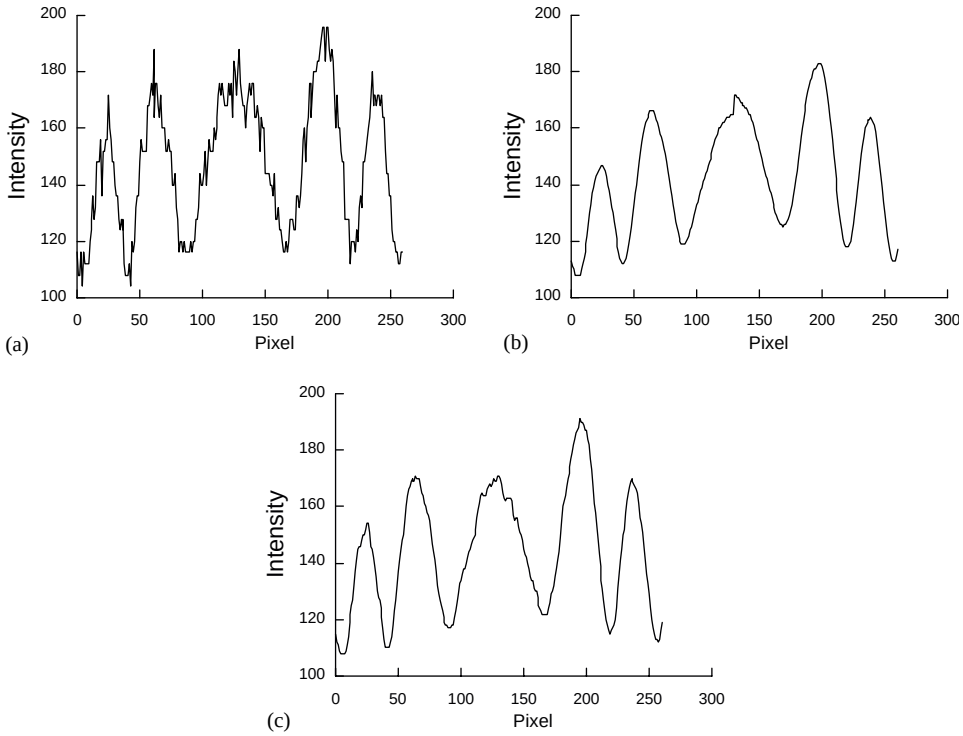

Fig. 2. The grayscale distribution in one section of the interferogram (a) original grayscale distribution of the holographic fringe pattern, (b) grayscale distribution after using a general average filter and, (c) grayscale distribution after using the anisotropic average filter.

fringe direction information can be used to apply a one-dimensional median or average filter to the fringe pattern and derivative sign binary map. In previous applications, the one-dimensional filter has been referred to as an anisotropic filter [15].

For an ideal fringe pattern the grayscale level gradient, over a neighboring area from each fringe, has minimum and maximum values tangent and normal to the fringe direction, respectively. Utilizing a one-dimensional median or average filter along the fringe tangent direction causes minimal blurring because the grayscales are almost equal in that direction. For a real fringe pattern with Gauss noise distribution, the one-dimensional filter is also an effective method for noise suppression.

After obtaining the fringe direction information, a grayscale image ranging from 0 to 255 provides the angle between the fringe tangent and the x-axis ($0^\circ \leqslant \gamma_r \leqslant 360^\circ$) at every point in the fringe pattern. A one-dimensional filter can be designed to remove noise along the local fringe direction according to16 possible directions as defined in Fig. 5(a) and (b). In general, a 5×5 window is the minimum acceptable subimage size for filtering or fringe direction determination. For a 5×5 window only 16

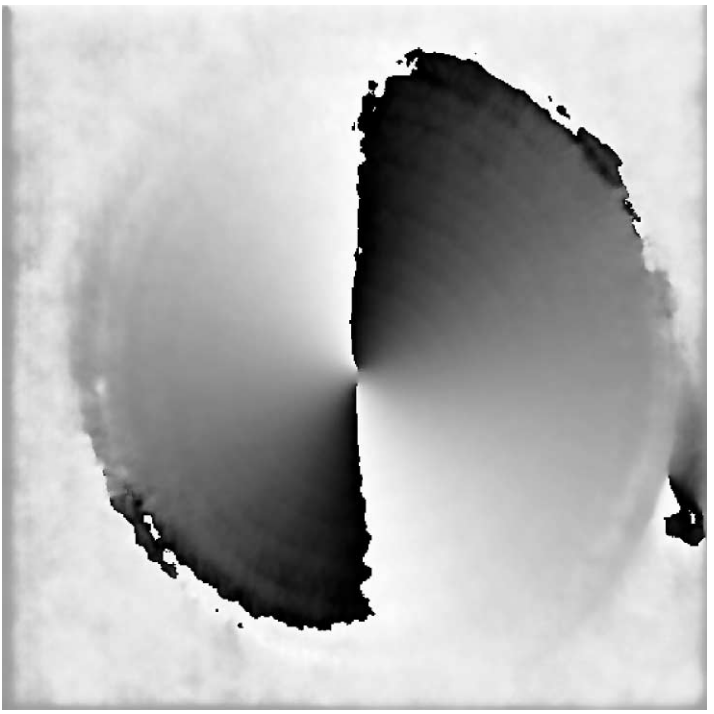

Fig. 3. The fringe orientation saw-tooth map (from $0^\circ \leqslant \alpha \leqslant 180^\circ$).

directions can be defined. As the fringe direction (γ_r) has 256 grayscale levels and there are a total of 16 possible directions, each of the 16 grayscale levels represents one of the 16 fringe directions.

Using the one-dimensional average filter, the grayscale of a current point is replaced by the average value of the grayscales in the neighboring area along the fringe tangent direction. The one-dimensional average operation can only be applied to fringe patterns and is not suitable for processing the derivative sign binary map since the binary map is described by only two values (0 and 255) and the average operation may define an invalid grayscale.

A one-dimensional median filter may be used for both fringe patterns and derivative sign binary maps. Using this method the grayscale of a current point is replaced by the middle of the sorted grayscales in the neighboring area along the fringe tangent. Of course, a combination of the median and average filters may be used for noise suppression. The median filter should always be used first to remove pulsed noise with large discrepancy in intensity from the primary grayscale. The grayscale distribution of the holographic interferogram in Fig. 1 is shown in Fig. 2(c) after performing one-dimensional median and average filters with the appropriate points (along the fringe direction) over a 5×5 neighborhood. As these anisotropic median and average filters are actually one-dimensional operations, they operate relatively faster than conventional median and average algorithms.

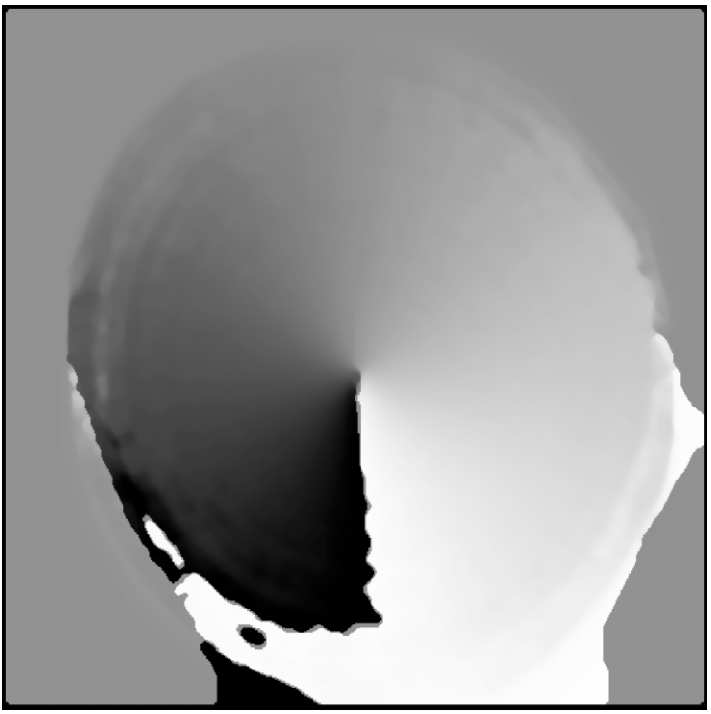

Fig. 4. The fringe direction map ($0^\circ \leqslant \gamma_r \leqslant 360^\circ$).

4. Continuous derivative sign binary map

Following application of the anisotropic filter for improving fringe quality, the fringe pattern transverse grayscale has a sinusoidal distribution, where the peak and valley points represent the light and dark points of the fringe pattern, respectively. These points could be identified from the locations where the derivative of the grayscale equals zero over a finite neighborhood of pixels in a specific direction. For a digital image, the location of peak (bright) and valley (dark) points defining the fringe center can be found from satisfying the conditions,

$$\text{Location}_{\text{peak}} \Rightarrow \text{Grayscale}_{i+1} - \text{Grayscale}_{i-1} = 0, \tag{6a}$$

$$\text{Location}_{\text{peak}} \Rightarrow \text{Grayscale}_{i-2} + \text{Grayscale}_{i+2} - 2\mathit{Grayscale}_i < 0, \tag{6b}$$

$$\text{Location}_{\text{valley}} \Rightarrow \text{Grayscale}_{i+1} - \text{Grayscale}_{i-1} = 0, \tag{7a}$$

$$\text{Location}_{\text{valley}} \Rightarrow \text{Grayscale}_{i-2} + \text{Grayscale}_{i+2} - 2\text{Grayscale}_i > 0. \tag{7b}$$

The derivative sign binary map may be obtained by applying Eqs. (6) and (7) along the fringe normal direction. In locations where

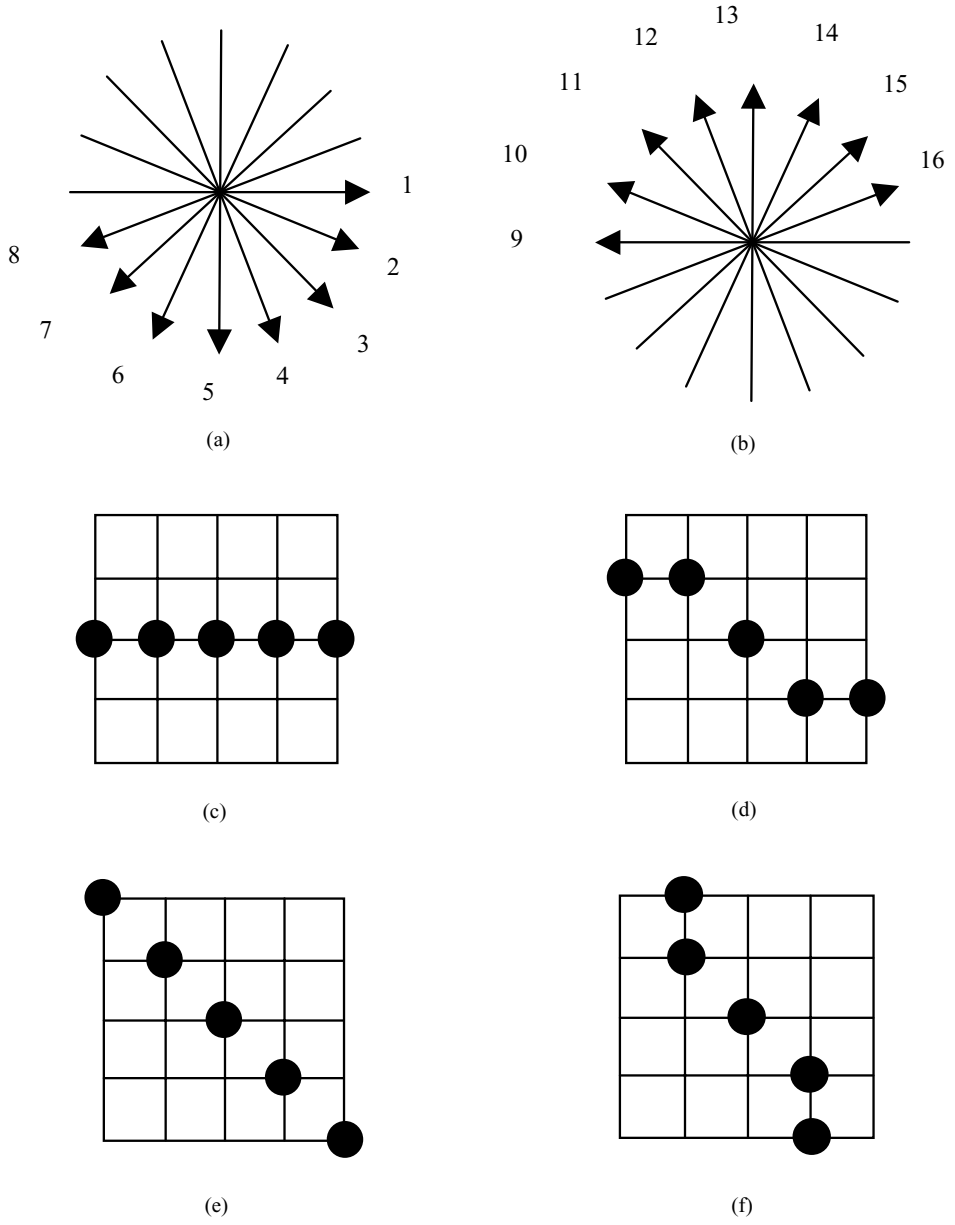

Fig. 5. Schematic diagrams and definitions for the local fringe directions (a) fringe direction definitions from 1 through 8, (b) fringe direction definitions from 9 through 16, (c) direction 1,(d) direction 2, (e) direction 3, and (f) direction 4.

$\text{Grayscale}_{i+1} - \text{Grayscale}_{i-1} < 0$ on the fringe patterns, the grayscale value is defined as zero and where $\text{Grayscale}_{i+1} - \text{Grayscale}_{i-1} \geqslant 0$ the grayscale value is defined as 255.

In practice, the fringe direction and its tangent are defined in terms of a restricted set of directions. A 5×5 sampling window with 16 possible directions was utilized to represent the local fringe directions of the interferogram (Fig. 1) as shown in Fig. 5(a) and (b). The first 4 directions are defined in Fig. 5(c)–(f). Note that the algorithm comprised of activities defined by Eqs. (6) and (7) should be performed normal to the fringe direction (γ_r) for maximum precision. Furthermore, the operations should be performed strictly according to the directions indicated by the vector definitions in Fig. 5(a) and 5(b). As a consequence, the grayscale difference at any point ($\text{Grayscale}_{i+1} - \text{Grayscale}_{i-1}$) obtained for a specific direction (e.g. direction 1) will have a sign difference from that of the opposite direction (e.g. direction 9). The derivative sign binary fringes with boundary representing the fringe intensity maximum and minimum are then obtained without a fringe direction jump. The derivative sign binary map for the holographic interferogram is shown in Fig. 6 following the application of the anisotropic median filter.

Fig. 6. The continuous derivative sign binary map.

5. Extracting fringe skeletons

The dark (light) fringe intensity centers can be detected from the boundaries of the derivative sign binary map using Eqs. (6b) and (7b). To extract the grayscale jump points, a neighboring differentiation algorithm is performed with the grayscale values according to

$$G_{i,j} = |G_{i,j} - G_{i,j-1}| + |G_{i,j} - G_{i-1,j}|. \tag{8}$$

Through application of Eq. (8) the grayscale of point (i,j) is replaced by the sum of the differences between its grayscale and that of its neighboring points in the x and y direction. Obviously, $G_{i,j}$ would remain zero if the point is located inside of the black or white zones and would be non-zero only if the point is located at the fringe boundary. In order to extract light and dark fringe skeletons separately, Eq. (6a) and (6b) andEq. (7a) and (7b) should be used. The skeletons defined at the dark (light) fringe centers of the interferogram in Fig. 1 are shown in Fig. 7. They provide a continuous definition of the fringe center with single point width and therefore provide a precise description

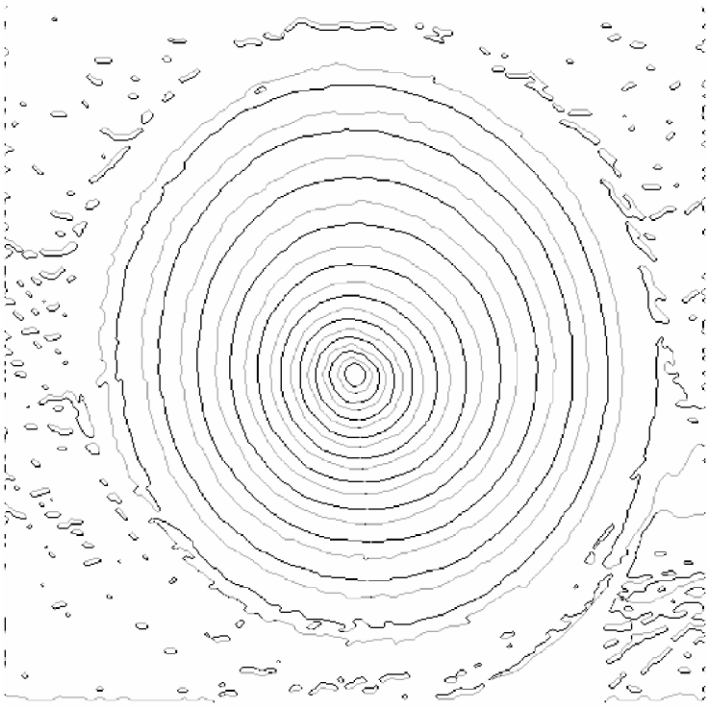

Fig. 7. Fringe skeletons obtained for the holographic interferogram (Fig. 1). The dark (light) fringe center is displayed with grayscale of 200 (100).

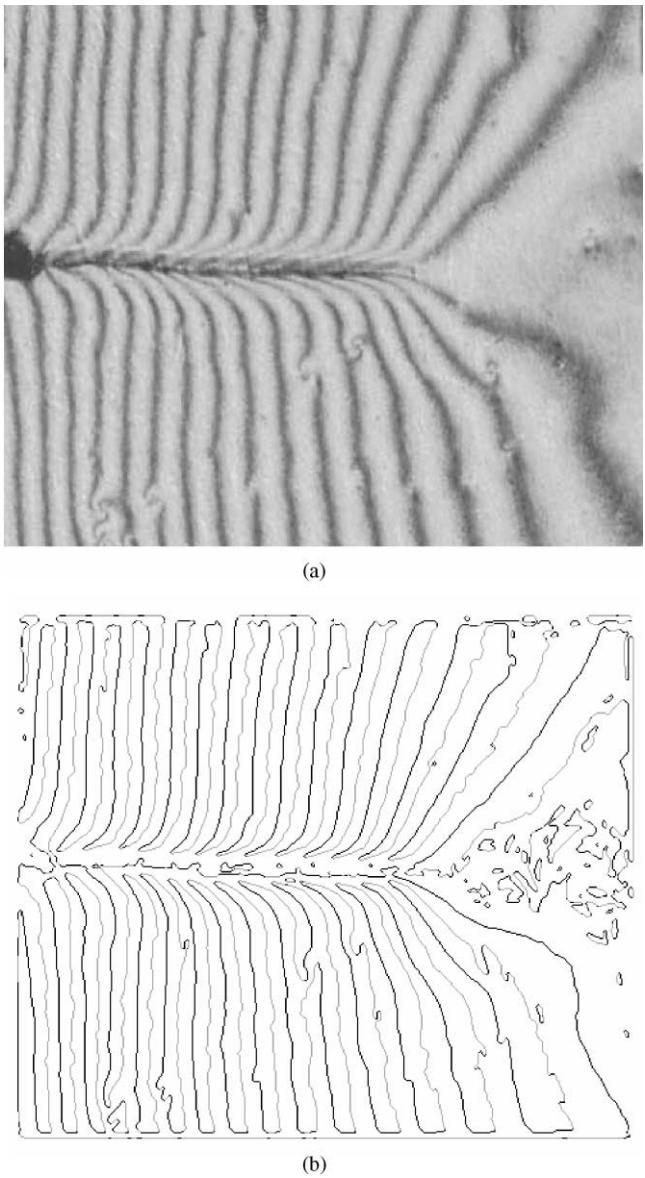

Fig. 8. The Moiré fringe field and skeletons corresponding to the displacement distribution near the crack tip during stable crack growth in a double cantilever beam of bovine dentin (a) fringe field and, (b) skeletons. The dark (light) fringe center is displayed with a grayscale of 200 (100).

of the displacement field. Another experimental fringe pattern obtained at the crack tip of a fracture specimen using Moiré interferometry is shown in Fig. 8(a). Processed using the improved derivative sign binary method, the fringe skeletons for this field are shown in Fig. 8(b).

6. Conclusion

A modified derivative sign binary method has been proposed which can be used to extract fringe skeletons precisely and automatically. The fringe direction mapping process described in this paper results in a unique relationship between the grayscale and fringe tangent direction with the range from 0° to 360°. The fringe direction map can then be used to obtain a continuous derivative sign binary map with boundary representing the fringe skeleton. Two different anisotropic (one-dimensional average and median) filters are also described which can be used with the fringe direction map for selectively improving the fringe skeleton quality with negligible blurring. The median filter can be applied to the derivative sign binary map as well to further improve the overall skeleton quality.

References

[1] Cline HE, Lorensen WE, Holik AS. Automatic Moiré contouring. Appl Opt 1984;23(10):1454–9.
[2] Zhang F, Shu M, Chen P. Digital image analysis system for photoelasticity. In: Chiang F, editor. Photomechanics and Speckle Metrology. Proceedings of the Society of Photo-Optical Instrumentation Engineers, vol. 814, 1987. p. 806–9.
[3] Becker F, Yu Y. Digital fringe reduction techniques applied to the measurement of three-dimensional transonic flow field. Opt Eng 1985;24(3):429–34.
[4] Kafri O, Ashkenaszi R. Line thinning algorithm for nearly straight Moiré fringes. Opt Eng 1986;25(3):495–8.
[5] Eichhorn N, Osten W. An algorithm for the fast derivation of line structures from interferograms. J Mod Opt 1988;35(10):1717–25.
[6] Chen TY, Taylor CE. Computerised fringe analysis in photomechanics. Exp Mech 1989;29(3):323–9.
[7] Ramesh K, Singh RK. Comparative performance evaluation of various fringe thinning algorithms in photomechanics. J Electron Imaging 1995;4(1):71–83.
[8] Tan H, Trolinger J D, Modarress D. An automated holographic interferometry data reduction system. In: Ponseggi BG, editor. High Speed Photography, Videography and Photonics IV, Proceedings of the Society of Photo-Optical Instrumentation Engineering, vol. 693, 1986. p. 161–5.
[9] Yu Q. Spin filtering processes and automatic extraction of fringe center lines from interferometric patterns. Appl Opt 1988;27(18):3782–4.
[10] Yu Q, Andreson K. Fringe-orientation maps and fringe skeleton extraction by the two-dimensional derivative-sign binary-fringe method. Appl Opt 1994;33(29):6873–8.
[11] Yatagai T, Nakadate S, Idesawa M, Saito H. Automatic fringe analysis using digital image processing techniques. Opt Eng 1982;21(3):432–5.
[12] Umezaki E, Tamakai T, Takahashi S. Automatic stress analysis of photoelastic experiment by use of image processing. Exp Tech 1989;13(6):22–7.
[13] Marroquin JL, Rodriquez-Vera R, Servin M. Local phase from local orientation by solution of a sequence of linear system. J Opt Soc Am 1998;15(6):1536–44.
[14] Castleman KR. Digital image processing. Englewood Hall, NJ: Prentice-Hall International, Inc., 1996.
[15] Winter H, Unger S, Osten W. The application of adaptive and anisotropic filtering for the extraction of fringe pattern skeletons. In: Osten W, Pryputniewicz RJ, editors. Fringe '89, Automatic Processing of Fringe Patterns, 1989. p. 158–66.